

## LETTER TO THE JOURNAL

# Oral transforming growth factor-beta receptor 1 inhibitor vactosertib promotes osteosarcoma regression by targeting tumor proliferation and enhancing anti-tumor immunity

Osteosarcoma is an aggressive malignant bone sarcoma common among children, adolescents, and young adults. Approximately 20% of patients present with pulmonary metastasis, and an additional 40% develop pulmonary osteosarcoma later. The survival outcome in patients with recurrent osteosarcoma and pulmonary osteosarcoma has not improved over many decades [1]. Transforming growth factor- $\beta$  (TGF- $\beta$ ) is a potent immunosuppressive molecule in the osteosarcoma tumor microenvironment (TME) known to suppress the function of cytotoxic T cells and natural killer (NK) cells and correlates with high-grade osteosarcoma and pulmonary osteosarcoma [2]. Vactosertib (TEW-7197) is a highly selective and potent small molecule inhibitor against Type 1 TGF- $\beta$  Receptor (activin receptor-like kinase 5; ALK5) [3]. Vactosertib is orally available and has 10 times the potency of galunisertib ( $IC_{50} = 11 \times 10^{-3} \mu\text{mol/L}$  vs.  $11 \times 10^{-2} \mu\text{mol/L}$ ) when tested in 4T1 [4], and is well tolerated with a manageable safety profile in adults, representing an attractive option in osteosarcoma [3].

TGF- $\beta$ 1 levels correlate with overall survival in osteosarcoma patients (Figure 1A). Vactosertib directly suppressed mouse osteosarcoma and human osteosarcoma cell line growth in a dose-dependent manner, with an  $IC_{50}$  of 0.79–2.1  $\mu\text{mol/L}$  (Figure 1B). Vactosertib ( $1 \times 10^{-1} \mu\text{mol/L}$ ) completely suppressed the TGF- $\beta$  signaling intermediate, p-Smad2, in mouse osteosarcoma and human osteosarcoma cells (Figure 1C). In contrast, other TGF- $\beta$ 1

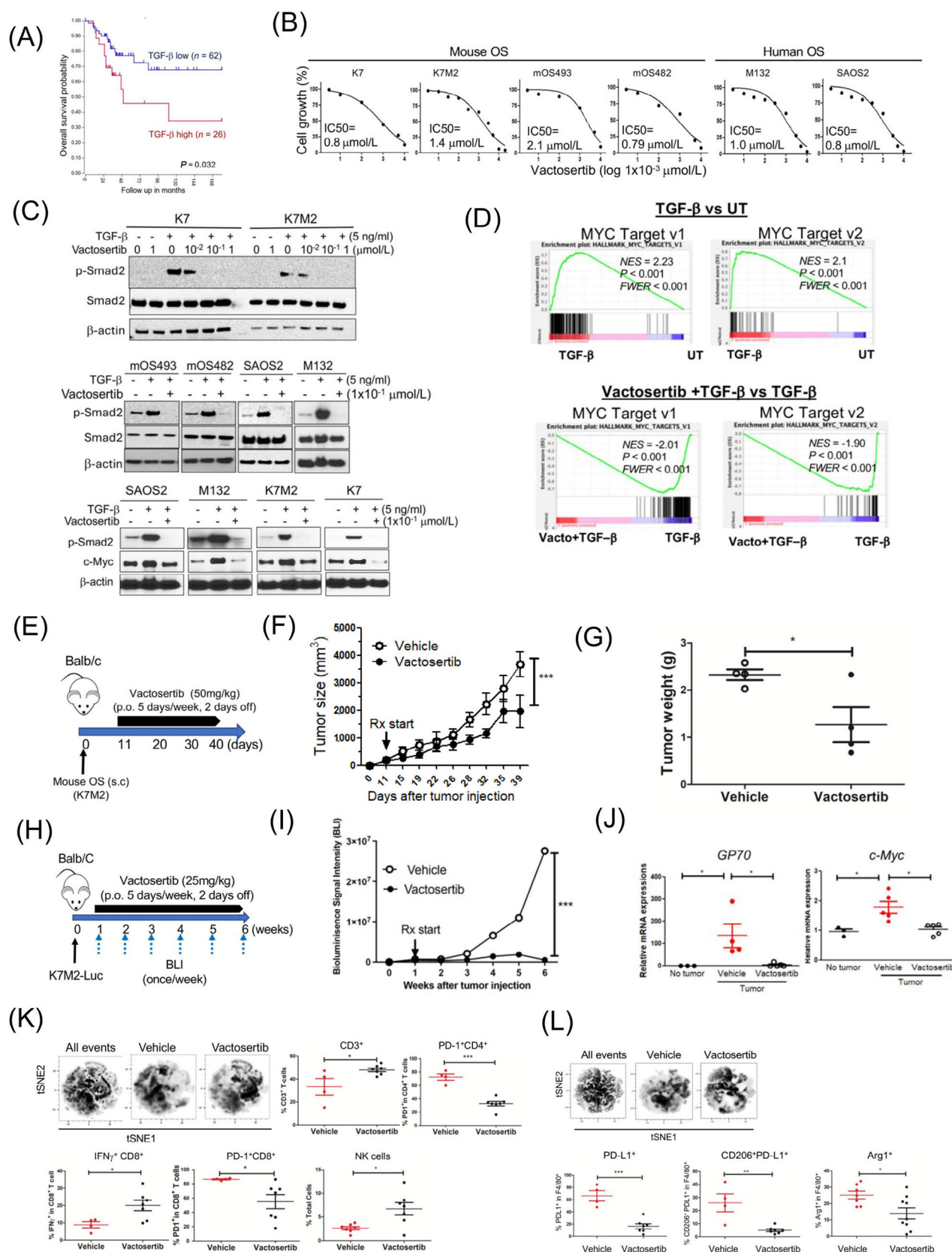
inhibitors, SB431542 and galunisertib, exhibited an  $IC_{50}$  of  $2.05 \times 10^3 \mu\text{mol/L}$  and 12  $\mu\text{mol/L}$ , respectively, and they were not able to suppress p-Smad2 at  $1 \times 10^{-1} \mu\text{mol/L}$  in SAOS2 cells (Supplementary Figure S1A–B). Vactosertib ( $1 \times 10^{-1} \mu\text{mol/L}$ ) treated SAOS2 cells displayed 35 upregulated and 72 downregulated genes, including decreased expression of Ephrin-2 (EFNB2), IL-11, and prostate transmembrane protein androgen induced1 (PMEPA1) which were all associated with osteosarcoma progression and metastasis (Supplementary Figure S2A) [5]. Gene Set Enrichment Analysis (GSEA) revealed 14 down-regulated gene sets, including Wnt Beta-catenin signaling, TGF- $\beta$ 1 and mammalian target of rapamycin complex 1 (mTORC1) signaling (Supplementary Figure S2B), with Myelocytomatosis (MYC) target genes among the most inhibited (Supplementary Figure S2B–C).

SAOS2 treated with TGF- $\beta$ 1 (5 ng/mL) alone most significantly increased c-Myc target genes, and vactosertib co-treatment with TGF- $\beta$ 1 significantly suppressed the same c-Myc target gene sets (Figure 1D). Expression of individual c-Myc target genes was independently confirmed using real-time reverse transcription-polymerase chain reaction (RT-PCR) (Supplementary Figure S2D). TGF- $\beta$ 1 (5 ng/mL) treatment alone also significantly increased c-Myc protein expression in SAOS2 cells, while a low dose of vactosertib ( $1 \times 10^{-1} \mu\text{mol/L}$ ) completely abolished TGF- $\beta$ 1-induced c-Myc expression in SAOS2 cells (Figure 1C, Supplementary Figure S2E). This inhibition was extended beyond SAOS2 into other human osteosarcoma and mouse osteosarcoma cell lines (Figure 1C). Volcano plots identified *PMEPA1*, *LTBP1*, *IL-11* and *JUNB* as genes most significantly increased by TGF- $\beta$ 1 and suppressed by vactosertib co-treatment in SAOS2 cells (Supplementary Figure S2F–G). Previous studies have shown these genes to be involved in tumor progressions and metastasis, and JUNB has also been reported to bind the promoter of c-Myc and regulate its expression [6].

**Abbreviation:** BLI, bioluminescent imaging; c-Myc, cellular-Myelocytomatosis; FACS, fluorescence-activated cell sorting; hOS, human osteosarcoma; ICB, immune checkpoint blockade; mOS, murine osteosarcoma; mTORC, mammalian target of rapamycin complex 1; pOS, pulmonary metastatic osteosarcoma; PD-1, programmed death 1; PD-L1, programmed death-ligand 1; p.o., per oral; RNA-seq, RNA sequencing; RT-PCR, real-time reverse transcription-polymerase chain reaction; s.c., subcutaneous; TAMs, tumor-associated macrophages; TGF- $\beta$ 1, transforming growth factor-beta 1; TME, tumor microenvironment; tSNE, t-distributed stochastic neighbor embedding.

This is an open access article under the terms of the [Creative Commons Attribution-NonCommercial-NoDerivs](https://creativecommons.org/licenses/by-nc-nd/4.0/) License, which permits use and distribution in any medium, provided the original work is properly cited, the use is non-commercial and no modifications or adaptations are made.

© 2024 The Authors. *Cancer Communications* published by John Wiley & Sons Australia, Ltd. on behalf of Sun Yat-sen University Cancer Center.



To test direct TGF- $\beta$  inhibition of osteosarcoma growth in vivo, we administered vactosertib (50 mg/kg, 5 days/week, per os [p.o.]) starting 14 days after SAOS2 inoculation (subcutaneous [s.c.]) into NK-depleted Nude mice (Supplementary Figure S3A) and observed blunted tumor growth in vactosertib treated group (Supplementary Figure S3B). Similarly, improved survival rates, smaller tumor volume and reduced metastasis were observed in SAOS2-bearing NSG mice treated with vactosertib after almost 3 months (Supplementary Figure S3C-F), accompanied by a reduction in p-Smad2 (Figure S3G) and c-Myc mRNA expression in residual tumors in vivo (Supplementary Figure S3H). As c-Myc amplification has been reported in metastatic and chemo-resistant osteosarcoma [7], we tested vactosertib on 143B, a c-Myc amplified human osteosarcoma with high c-Myc at baseline (Supplementary Figure S3I). 143B growth was not inhibited by a wide dose range of vactosertib ( $10 \times 10^{-3}$   $\mu$ mol/L to  $10 \times 10^{-6}$   $\mu$ mol/L) in vitro (Supplementary Figure S3J). Although vactosertib potentially shut down pSmad2, ERK phosphorylation remained unchanged in 143B (Supplementary Figure S3I). Interestingly, vactosertib could not inhibit 143B tumor in

NSG mice in vivo (Supplementary Figure S3K) but was able to do so in nude mice (Supplementary Figure S3L), suggesting a tumor-extrinsic effect of vactosertib such as through enhancement of NK cell function [8].

To assess the osteosarcoma-extrinsic effects of vactosertib on the immune landscape of the primary tumor sites, we employed a K7M2 model in BALB/c mice (Figure 1E). Vactosertib treatment (50 mg/kg, 5 days/week, p.o.) significantly inhibited K7M2 tumor growth (Figure 1F-G). While no statistically significant differences were observed in the percentage of the CD45, CD11b or MDSC (Ly6C<sup>lo</sup>Ly6G<sup>Hi</sup>, Ly6C<sup>Hi</sup>Ly6G<sup>-</sup>) cell populations (Supplementary Figure S3M), M2-like tumor-associated macrophages (TAMs) (CD11b<sup>+</sup>F4/80<sup>+</sup>Arg<sup>+</sup>PD-L1<sup>+</sup>) were significantly suppressed by vactosertib (Supplementary Figure S3M). Using a pulmonary osteosarcoma model where BALB/c mice were inoculated with  $1 \times 10^6$  K7M2-Luc cells (i.v.) and treated with vactosertib via oral gavage starting 7 days later (Figure 1H), vactosertib-treated mice exhibited a dramatic inhibition of pulmonary osteosarcoma burden with a suppressed tumor c-Myc expression (Figure 1I-J). At a higher dose, vactosertib was efficacious

**FIGURE 1** Vactosertib inhibits osteosarcoma cell growth in vitro and in vivo. (A) Kaplan-Meier overall survival curves of high-grade osteosarcoma patients and their expression of TGF- $\beta$ 1 in clinical biopsies. Data were obtained from “R2: Genomics analysis and visualization platform” [<http://r2.amc.nl>]. Datasets provided by Kuijter ( $n = 88$ ). The red line indicates high expression of TGF- $\beta$ 1 ( $n = 26$ ), while the blue line indicates low expression of TGF- $\beta$ 1 ( $n = 62$ ). Kaplan-Meier curves showed worse overall survival rates of osteosarcoma patients with high TGF- $\beta$  expression compared to patients with low TGF- $\beta$  expression ( $P = 0.032$ ). (B) Effects of vactosertib on osteosarcoma proliferation. Various doses of vactosertib ( $10 \times 10^{-3}$   $\mu$ mol/L to  $10 \mu$ mol/L) were incubated with mOS (K7, K7M2, mOS493, and mOS482) or hOS (M132 and SAOS2). Cell growth was quantified over a 4-day period using the IncuCyte Imaging System. The non-linear regression (curve fit) equation was calculated using GraphPad prism ( $n = 5$ /group). (C) Vactosertib inhibits TGF- $\beta$ 1 signaling pathway in osteosarcoma cells. Various doses of vactosertib ( $1 \times 10^{-2}$   $\mu$ mol/L to  $1 \mu$ mol/L) were used to treat in K7, K7M2, mOS493, mOS482, SAOS2 and M132 cells 15 minutes before TGF- $\beta$ 1 (5 ng/ml) treatment. 1 hour after TGF- $\beta$ 1 treatment, cells were harvested and p-Smad2, Smad2 and  $\beta$ -actin expressions were measured by Western blot analysis. TGF- $\beta$ 1 (5 ng/ml) or TGF- $\beta$ 1 (5 ng/ml) / vactosertib (Vacto) ( $1 \times 10^{-1}$   $\mu$ mol/L) were used to treat various osteosarcoma (SAOS2, M132, K7M2, K7) for 24 hours and c-Myc and  $\beta$ -actin protein expressions were measured by Western blot analysis. (D) RNA-sequencing analysis of human osteosarcoma (SAOS2) cells after TGF- $\beta$ 1 (5 ng/ml), TGF- $\beta$ 1+ vactosertib ( $1 \times 10^{-1}$   $\mu$ mol/L) or untreated (UT) for 24 hours. GSEA enrichment plot of c-Myc target v1 and v2 pathway in TGF- $\beta$ 1 treatment versus untreated and in TGF- $\beta$ 1 + Vacto vs TGF- $\beta$ 1.  $P$  values are  $< 0.001$  and  $FWER$  is  $< 0.001$  for both analyses. (E-G) Vactosertib inhibited OS cell growth in vivo. (E) BALB/c mice were inoculated with  $1 \times 10^6$  K7M2 (s.c.) on Day 0, and then treated with vehicle (p.o.) or vactosertib (50 mg/kg, p.o. 5 days/week) starting on day 11. (F) tumor sizes were measured by caliper.  $n = 4$ , \*\*\* $P < 0.001$  using a two-way ANOVA between groups followed by post-hoc Bonferroni's multiple comparison tests. (G) Tumor weight was measured ( $n = 4$ ). (H-J) Vactosertib inhibits mouse pOS development in vivo. (H) BALB/c mice were inoculated with  $1 \times 10^6$  K7M2-Luc (i.v.) on day 0, and then treated with vehicle (p.o.) or vactosertib (25 mg/kg p.o. 5 days/week) starting on day 7. (I) BLI was measured once a week. (J) Relative mRNA expression of GP70 and c-Myc in lung samples of the vehicle or vactosertib-treated mice on day 42 days after tumor injection compared with that of control lungs of no tumor-bearing mice.  $n = 5$ /group, \* $P < 0.05$  using an unpaired two-tailed t-test. (K-L) BALB/c mice were inoculated with  $1 \times 10^6$  K7M2-Luc (i.v.) on Day 0, and then treated with vehicle (p.o.) or vactosertib (50 mg/kg, p.o. 5 days/week) starting on day 28 (4 weeks). Ten weeks after tumor injection, lung samples were collected. (K) FACS was performed and expression of CD3, CD4, CD8, NK (CD49b), PD-1 and IFN $\gamma$  was determined by FACS. Unbiased immune cell profiling on 5000 live CD45.2 cells by t-SNE analysis was performed. tSNE density plots of live cells in vehicle or vactosertib-treated samples. The frequency of T cell markers by conventional FACS analysis. Vehicle  $n = 4$ , vactosertib  $n = 7$  \* $P < 0.05$ , \*\*\* $P < 0.001$ , using an unpaired two-tailed t-test. (L) Examined for expression of F4/80, PD-L1, CD206 and Arg1 by FACS. tSNE density plots of CD45.2<sup>+</sup> cells in vehicle or vactosertib-treated samples. The frequency of myeloid cell markers by conventional FACS analysis. Vehicle  $n = 4-7$ , vactosertib  $n = 7-9$ , \* $P < 0.05$ , \*\* $P < 0.01$  using an unpaired two-tailed t-test. Abbreviations: BLI, bioluminescent imaging; c-Myc, cellular-Myelocytomatosis; FACS, fluorescence-activated cell sorting; hOS: human osteosarcoma; p.o., per os; PD-1, Programmed death 1; PD-L1, programmed death-ligand 1; RNA-seq, RNA sequence; s.c., subcutaneous; TGF- $\beta$ 1, Transforming growth factor-beta 1; tSNE, t-distributed stochastic neighbor embedding; UT, untreated; Vacto, vactosertib.



in suppressing tumor growth even when starting late (3 weeks) at a higher tumor burden (Supplementary Figure S4A-C), accompanied by reduced lung metastasis (Supplementary Figure S4D-E). Interestingly, c-Myc expression in lung tissue was similar despite its clinical efficacy (Supplementary Figure S4F), implying a critical role for enhanced anti-tumor immunity *in vivo*.

Poor response to osteosarcoma therapy is correlated with low CD8<sup>+</sup> T cells and IFN $\gamma$  expression [9]. To elucidate how vactosertib affects the *in vivo* immune landscape, we performed multiparametric flow cytometry (FACS) with tSNE analysis of lung tissues (Supplementary Figure S5A). The analysis showed vactosertib-exposed TME contained significantly more CD3<sup>+</sup>, IFN<sup>+</sup>CD8<sup>+</sup> and NK cells, along with a decreased prevalence of PD1<sup>+</sup>CD8<sup>+</sup> T cells, PD1<sup>+</sup>CD4<sup>+</sup> T cells (Figure 1K) and Foxp3<sup>+</sup>CD4<sup>+</sup> T cell subsets (data not shown). Vactosertib exposure resulted in the accumulation and deep infiltration of NK cells within the tumors while they were scattered and largely confined to the tumor periphery in vehicle controls (Supplementary Figure S6).

Examination of the myeloid cells (Supplementary Figure S5B) also showed a clear difference upon vactosertib treatment, with a suppression of M2-like TAMs expressing PD-L1<sup>+</sup>, CD206<sup>+</sup>PD-L1<sup>+</sup>, and Arg1<sup>+</sup> markers (Figure 1L). Similar to TAMs, vactosertib also diminished F4/80<sup>+</sup> CD11b<sup>+</sup>Ly6G<sup>+</sup>Ly6C<sup>+</sup> and CD11b<sup>+</sup>Ly6G<sup>+</sup>Ly6C<sup>+</sup> myeloid cells (data not shown), further supporting vactosertib as enhancing anti-tumor immunity in pulmonary osteosarcoma TME. Finally, we tested co-treatment with vactosertib and  $\alpha$ PD-1/  $\alpha$ PD-L1 mAb for synergy against osteosarcoma *in vivo* (Supplementary Figure S7). Vactosertib alone inhibited osteosarcoma tumor growth as well as  $\alpha$ PD-L1 mAb alone or in combination. Interestingly, in agreement with ongoing disappointing clinical observation in osteosarcoma patients receiving  $\alpha$ PD-1 therapies [10], we did not observe a therapeutic efficacy with  $\alpha$ PD-1 mAb *in vivo*. As vactosertib significantly reduced PD-1<sup>+</sup> T-cells and suppressed PD-L1<sup>+</sup> macrophages, the lack of synergistic effects of vactosertib and ICB may be explained by the reduction in the numbers of these cells. The exact mechanism(s) for this lack of clinical efficacy by targeting PD-1 in osteosarcoma await additional studies.

Based on our current study, a multi-continent (US, Europe, Asia), multi-center phase I/II clinical trial (NCT05588648) with vactosertib monotherapy for osteosarcoma is actively enrolling. The application of vactosertib as an adjuvant to additional cellular therapy and immune-modulating approaches for osteosarcoma and other cancers awaits thoughtful exploration, such as inclusion in protocols targeting early-stage and high-risk disease. Taken together, inhibition of TGF- $\beta$  signaling could be an effective therapeutic strategy against pul-

monary osteosarcoma through a multi-pronged approach that targets tumor intrinsic and extrinsic factors to achieve optimal immune-effector functions and maximal clinical response.

## AUTHOR CONTRIBUTIONS

Sung Hee Choi and Alex Y. Huang conceptualized the project. Sung Hee Choi, Jay T. Myers, Suzanne L. Tomchuck, Melissa Bonner, Saada Eid, Daniel T. Kingsley, Kristen VanHeyst, and Byung-Gyu Kim performed experiments and analyzed data. Sung Hee Choi wrote the original draft of the manuscript. Jay T. Myers, Suzanne L. Tomchuck, Melissa Bonner, Saada Eid, Daniel T. Kingsley, Kristen VanHeyst, Seong-Jin Kim, Byung-Gyu Kim, and Alex Y. Huang reviewed and edited the manuscript. Alex Y. Huang acquired funding for the project. All authors have read and agreed to the published version of the manuscript.

## ACKNOWLEDGMENTS

We would like to thank the members of Alex Y. Huang's lab for their helpful discussion.

## CONFLICT OF INTERESTS STATEMENT

S.J.K declares a personal financial interest as a shareholder in TheragenEteX and Medpacto Inc. and is an employee of Medpacto Inc..

## FUNDING INFORMATION

This research was supported by the National Cancer Institute (R03CA273468, R03CA259901, P30CA043703, T32GM007250, T32CA059366, and K12CA076917), St. Baldrick's Foundation, Hyundai Hope-on-Wheels Scholar Hope Grant, Andrew McDonough B+ Foundation, Curing Kids Cancer, MIB Agents, Sarcoma Foundation of America, Sam Day Foundation, Children's Cancer Research Fund, Center for Pediatric Immunotherapy at Rainbow, and a sponsored research agreement from MedPacto, Inc. who provided vactosertib for both *in vitro* and *in vivo* experiments.



## DATA AVAILABILITY STATEMENT

Datasets generated and analyzed in this study are available from the corresponding author upon request in accordance with institutional data sharing policy.

## ETHICS APPROVAL AND CONSENT TO PARTICIPATE

All animal experiments were performed and monitored with strict adherence to protocols in accordance with institutional guidelines and with approval of the Institutional Animal Care and Use Committee (protocol # 2016-0067) at Case Western Reserve University School of Medicine and performed in accordance with the guidelines of the

American Association for Accreditation of Laboratory Animal Care and the NIH.

Sung Hee Choi<sup>1,2</sup>   
 Jay Thomas Myers<sup>1</sup>  
 Suzanne Louise Tomchuck<sup>1</sup>  
 Melissa Bonner<sup>3</sup>  
 Saada Eid<sup>1</sup>  
 Daniel Tyler Kingsley<sup>3</sup>  
 Kristen Ashley VanHeyst<sup>1,2</sup>  
 Seong-Jin Kim<sup>4</sup>  
 Byung-Gyu Kim<sup>1,2</sup>  
 Alex Yee-Chen Huang<sup>1,2,3,5</sup> 

<sup>1</sup>Department of Pediatrics, Case Western Reserve University  
 School of Medicine, Cleveland, Ohio, USA

<sup>2</sup>Case Comprehensive Cancer Center, Case Western Reserve  
 University School of Medicine, Cleveland, Ohio, USA

<sup>3</sup>Department of Pathology, Case Western Reserve University  
 School of Medicine, Cleveland, Ohio, USA

<sup>4</sup>MedPacto Inc., Seoul, Republic of Korea

<sup>5</sup>Center for Pediatric Immunotherapy, Angie Fowler AYA  
 Cancer Institute, UH Rainbow Babies and Children's  
 Hospital, Cleveland, Ohio, USA

### Correspondence

Sung Hee Choi, PhD, Department of Pediatrics, Case  
 Western Reserve University, Wolstein Research Building,  
 Room 6401, 2103 Cornell Road, Cleveland, Ohio 44106,  
 USA.

Email: [sxc224@case.edu](mailto:sxc224@case.edu)

Alex Yee-Chen Huang, MD, PhD, Department of  
 Pediatrics, Case Western Reserve University, Wolstein  
 Research Building, Room 6528, 2103 Cornell Road,  
 Cleveland, Ohio 44106, USA.

Email: [ayh3@case.edu](mailto:ayh3@case.edu)

### ORCID

Sung Hee Choi  <https://orcid.org/0000-0002-8102-5538>

Alex Yee-Chen Huang  <https://orcid.org/0000-0002-5701-4521>

### REFERENCES

1. Petrilli AS, de Camargo B, Filho VO, Bruniera P, Brunetto AL, Jesus-Garcia R, et al. Results of the Brazilian Osteosarcoma Treatment Group Studies III and IV: prognostic factors and impact on survival. *J Clin Oncol*. 2006;24(7):1161–1168.
2. Xu S, Yang S, Sun G, Huang W, Zhang Y. Transforming growth factor-beta polymorphisms and serum level in the development of osteosarcoma. *DNA Cell Biol*. 2014;33(11):802–806.
3. Kim BG, Malek E, Choi SH, Ignatz-Hoover JJ, Driscoll JJ. Novel therapies emerging in oncology to target the TGF-beta pathway. *J Hematol Oncol*. 2021;14(1):55.
4. Son JY, Park SY, Kim SJ, Lee SJ, Park SA, Kim MJ, et al. EW-7197, a novel ALK-5 kinase inhibitor, potently inhibits breast to lung metastasis. *Mol Cancer Ther*. 2014;13(7):1704–1716.
5. de Oliveira Rodrigues MT, Pereira da Silva L, Pogue RE, de Carvalho JL, Motoyama AB, de Alencar EST, et al. Induced resistance to ifosfamide in osteosarcoma cells suggests a more aggressive tumor profile. *Biochem Biophys Rep*. 2022;32:101357.
6. Garces de Los Fayos Alonso I, Liang HC, Turner SD, Lagger S, Merkel O, Kenner L. The Role of Activator Protein-1 (AP-1) Family Members in CD30-Positive Lymphomas. *Cancers (Basel)*. 2018;10(4):93.
7. Chen D, Zhao Z, Huang Z, Chen DC, Zhu XX, Wang YZ, et al. Super enhancer inhibitors suppress MYC driven transcriptional amplification and tumor progression in osteosarcoma. *Bone Res*. 2018;6:11.
8. Wong DP, Fritz CE, Feinberg D, Huang AY, Parameswaran R. p35 is a Crucial Player in NK-cell Cytotoxicity and TGFbeta-mediated NK-cell Dysfunction. *Cancer Res Commun*. 2023;3(5):793–806.
9. Yang H, Zhao L, Zhang Y, Li FF. A comprehensive analysis of immune infiltration in the tumor microenvironment of osteosarcoma. *Cancer Med*. 2021;10(16):5696–5711.
10. Boye K, Longhi A, Guren T, Lorenz S, Naess S, Pierini M, et al. Pembrolizumab in advanced osteosarcoma: results of a single-arm, open-label, phase 2 trial. *Cancer Immunol Immunother*. 2021;70(9):2617–2624.

### SUPPORTING INFORMATION

Additional supporting information can be found online in the Supporting Information section at the end of this article.